Deuteron n.m.r. study of chain motion in solid polyethylene

D. Hentschel, H. Sillescu and H. W. Spiess
Institut für Physikalische Chemie der Universität Mainz, Sonderforschungsbereich 41 Chemie und Physik der Makromoleküle, Jakob-Welder-Weg 15, D-6500 Mainz, W. Germany
(Received 5 August 1983)

The chain motion in the amorphous regions in linear polyethylene is studied by exploiting various ^2H n.m.r. pulse methods. The experimental techniques employed are described in considerable detail. In particular, the solid echo- and the spin alignment spectra are recorded over a wide range of temperatures (123–393 K) as a function of the pulse spacings. In addition the spin–lattice relaxation times of both polymerization and alignment are given for the crysralline as well as the amorphous regions. The data are analysed in terms of highly constrained conformational motions which generate an exchange of C–H bond directions between 2, 3, or all 4 tetrahedral sites on a diamond lattice. Thus in the temperature interval from the γ-relaxation up to $\sim$200 K only 2 sites are accessible, whereas a third site is appreciably populated at room temperature. Between 330 K and the melting point the number of conformations accessible to the chain must be high enough to lead to an increasingly isotropic 4 site exchange. The motion remains highly constrained and localized, however, up to the melting region as shown by the analysis of the spin-alignment spectra. The intensity ratio of the deuteron n.m.r. signals from the rigid crystalline and the mobile amorphous regions, respectively, yields the crystallinity of the sample as a function of temperature in remarkable agreement with the results obtained by X-rays. Finally, frequency dependent relaxation of spin alignment due to torsional oscillations of the chains in the crystalline regions is observed and analysed.

(Keywords: ^2H nuclear magnetic resonance; chain motion; polyethylene)

INTRODUCTION

The investigation of molecular motion in semicrystalline polymers by various relaxation methods has led to a better understanding of mechanical properties, but has also left many problems unsolved. In the endeavour to clarify the situation, polyethylene (PE) has become a model substance, in particular, since the fraction of mobile chains can be varied over a wide range by different sample preparation techniques or by introducing chain branching. However, this entails the additional problems of side chain motion, and of relating molecular motion with molecular morphology.

Advantages of ^2H n.m.r.

^2H n.m.r. has two particular features that make it a unique probe for molecular motion in solid polymers[1]:

(1) Any correlation time or correlation function extracted from an analysis of spin relaxation times, line shapes, or the response to appropriate pulse sequences is related solely with the reorientation of C–^2H bonds.

(2) In processes where the C–^2H bond is exchanged between a small number of possible orientations ^2H n.m.r. provides detailed information upon the type of the process. Thus, we will show that there is a wide temperature range where the γ-process in PE is governed by an exchange of C–H bonds between only 2 orientations until, at higher temperatures, a 3rd and 4th orientation become accessible[2]. This information rules out many speculations published in the past on this basis of relaxation experiments that yield only correlation times of basically unspecified processes. A further advantage of ^2H n.m.r. pertaining to semicrystalline polymers is the possibility of separating the contributions of mobile and 'rigid' deuterons since the n.m.r. signal of the latter can be largely saturated due to the much longer spin–lattice relaxation time T_1 (see below).

Molecular motion in PE as revealed by other techniques

PE exhibits three main relaxation processes[3,4]: The α process is related with chain motions in the crystalline domains, and influences most n.m.r. observables only at temperatures above $\sim$330 K[5]. The β process is most pronounced in branched PE and is found to be weak or absent in linear PE[3–6]. Since our n.m.r. study is restricted to a sample of linear PE of high crystallinity we postpone a thorough discussion of the β process to a future investigation. The γ process has been shown to occur only in the amorphous regions of PE[6,7]. Investigations of thermal expansion by density[7] and small angle X-ray scattering[8] measurements have led to the conclusion that the γ process is associated with a glass transition at $T_g \sim 130$ K. Other authors have placed T_g at higher temperatures[9–11], arguing that the γ process does not correspond to a glass transition since the increase of specific heat around 130 K is much smaller than expected by comparison with amorphous polymers above T_g[11]. There has been ample evidence that the γ process is related with localized conformational transitions only, e.g.,

0032-3861/84/081078-09$03.00

trans–gauche[12], kink[13] or crankshaft[14] motions. These interpretations are supported by a rather extensive dielectric study of partially oxidized or chlorinated PE[15]. The authors find that only 10–20% of the C=O or C–Cl dipoles in the amorphous regions participate in the γ relaxation even in low density PE with crystallinities below 40%, and they argue that this behaviour can only be explained by localized motions thus ruling out the long range cooperative motions typical of a glass process. The primary information of these dielectric relaxation experiments pertains to the motion of chain defects carrying a dipole moment, their main conclusions are supported, however, by our ^{2}H n.m.r. study discussed below, where the motion of intact chains is monitored directly.

There have been many ^{1}H and ^{13}C n.m.r. studies of PE providing partial information upon molecular motion. Though excellent reviews of the ^{1}H work have been given[5,6] we wish to summarize some results along with those of ^{13}C in order to ease comparison with our ^{2}H data. In various line-shape studies of ^{1}H n.m.r. spectra in PE the motionally narrowed portion of the spectrum has been separated from the 'rigid' portion by assuming that the latter coincide with the spectrum of high crystalline PE at low temperature[5] by adopting some particular shape function that approximates the spectrum in crystalline PE[16,17]. The motionally narrowed spectrum is described by one[18], two[5,16] or more[17,19] components attributed to different motional processes on the basis of qualitative considerations, in particular, by analysing the dependence of line-widths upon temperature and crystallinity. Comparison of the 2nd and 4th moment of the line-shape in ordered (drawn) PE samples allowed for comparison with model calculations of the moments for particular motional processes[6,20]. The authors conclude that the decrease of the 2nd moment between 80 and 300 K cannot be explained by kink motion alone. Kimmich and collaborators[11,21] have analysed ^{1}H spin–lattice relaxation times T_1 in terms of a defect diffusion model that implies a γ process by kink-like motions in PE. However, their results do not exclude motions where C–H bonds are exchanged between more than 2 orientations. They have measured the frequency dependence of T_1 at different temperatures and their experimental data apply basically to the dynamics of *trans–gauche* conformational transitions within the amorphous regions of PE. The advent of proton decoupled ^{13}C n.m.r. in solids has provided the possibility of studying molecular motion by its influence upon the chemical shift anisotropy of ^{13}C[23–25]. The results of applications to PE[24,25] are in qualitative agreement with those of ^{1}H and ^{2}H n.m.r. However, local fluctuations of the magnetic susceptibility due to heterogeneities inherent in semi-crystalline polymers cause additional line broadenings that depend upon the morphology of the sample investigated[24]. Furthermore, a quantitative analysis of motionally narrowed ^{13}C spectra is complicated by the fact that the chemical shift tensors differ for ^{13}C nuclei in *trans* and *gauche* positions and due to intermolecular contributions[26].

Outline of paper

In the present paper we first describe the experimental techniques applied in the ^{2}H n.m.r. study of molecular motion in PE, then we report the experimental results and their analysis in terms of various motional models. This section is followed by a discussion where we try to avoid arguments that presuppose the reader's acquaintance with advanced n.m.r. theory.

EXPERIMENTAL

Sample preparation

Fully deuterated linear PE ($M_w = 100\,000$, $M_w/M_n = 10$) was obtained from Merck, Darmstadt. About 1 g was melted at 430 K in the n.m.r. sample tube 8 mm in diameter, isothermally crystallized at 395.5 K for 180 h, and sealed under vacuum. It should be noted that the melting point of PED is 6 K below that of PEH if both samples are crystallized at equal undercooling.[27]

N.m.r. experiments

The ^{2}H n.m.r. data were obtained at 55 MHz on a Bruker SXP spectrometer with an Oxford Instruments 8.5 T magnet. The home built probe head could be used for variable temperatures between 110 and 450 K, the temperature gradient and stability was ~0.5 K over the sample size[29]. The following n.m.r. variables were measured by selecting particular pulse sequences (see *Figure 1*):

Solid echo: The pulse sequence BC generates a solid echo at τ_1 after pulse C, and an 'unwanted' FID that can be removed[31] as described below. The Fourier transforms (FT) of the solid echo decay yields the fully relaxed spectra shown below, cf. *Figure 4*. The repetition time was chosen $5 \times T_1^c$, the spin–lattice relaxation time of the crystalline deuterons whereas $\tau_1 = 20$ μs is small in comparison with T_2^a, the spin–relaxation time of the mobile deuterons.

Spin alignment echo[31]: The pulse sequence BCD generates an echo at τ_1 after pulse D. The echo amplitude recorded as a function of τ_2 yields the spin alignment relaxation time T_{1Q}^c of the crystalline deuterons (see *Figure 2*) provided $\tau_1 \gg T_2^a$ whereby the signal of the mobile deuterons is suppressed. The FT of the spin–alignment echo decay yields spectra as shown in *Figure 10*.

Saturation recovery n.m.r. signals: The pulse sequence A consisting of five 90° pulses separated by ~2 ms was applied in order to saturate the nuclear magnetization. If the waiting time τ_0 prior to application of the BC sequence is sufficiently short ($\tau_0 \ll T_1^c$) the solid echo corresponds only to the mobile deuterons. The FT spectra shown below in *Figures 6, 7,* and *8* are recorded under these conditions. The relaxation times T_1^a and T_1^c shown in *Figure 2* have been obtained by recording the solid echo amplitude as a function of τ_0, and by decomposing this function in exponentials. In the same fashion, the

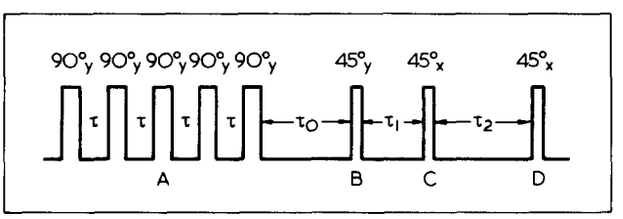

Figure 1 Pulse sequences for measuring n.m.r. spectra and relaxation times as described in the text

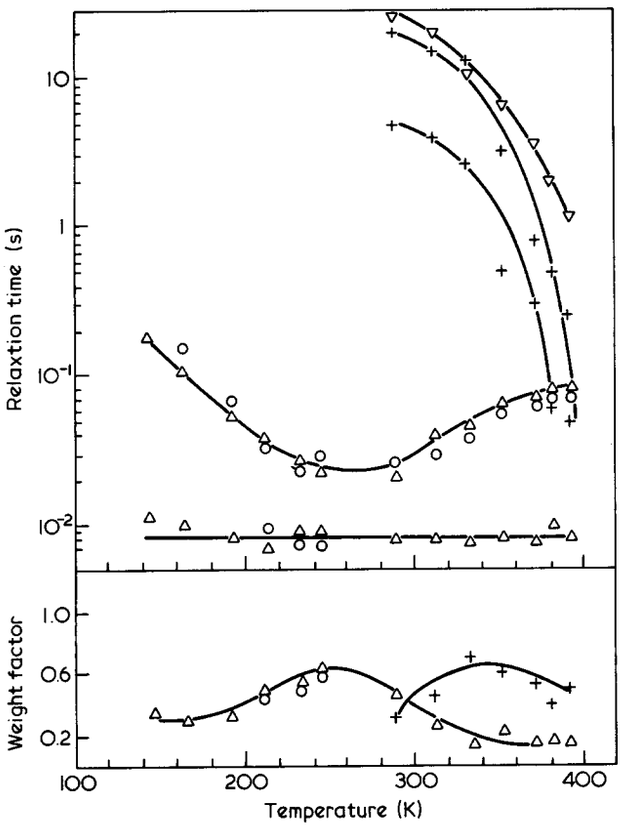

Figure 2 Spin–relaxtion times of rigid (index c) and mobile (index a) deuterons in the crystalline and amorphous regions of polyethylene: (○) T_1^a, (△) T_1^c, (△)T_{1Q}^a, (+) T_{1Q}^c. The weight factors denote the fraction of deuterons contributing to the initial rapid portion of the non-exponential magnetization curves for determining T_1^a, T_{1Q}^a, and T_{1Q}^c, respectively (see text)

relaxation time T_{1Q}^a was obtained by recording the spin alignment echo amplitude as a function of τ_2 for fixed $\tau_1 = 20\ \mu s$ and $\tau_0 \ll T_{1Q}^c$ (see *Figure 2*). The *FT* spin alignment spectra shown in *Figure 7* were obtained under the same conditions.

Correction procedures: By chosing 45° pulses for the solid echo BC sequence the pulse length of 2 μs was sufficiently short for obtaining solid state ^2H spectra that were reduced in intensity by only about 10% at the outer edges. The distortion of the spectrum due to finite pulse length was accounted for by using the $\sin x/x$ correction[28], however, with an increased effective pulse length[29] of 2.54 μs for the 45° pulse that approximates the more elaborate correction calculated by Bloom and collaborators[30]. The ringing signal of the refocussing pulses C and D, respectively, was suppressed by π-shifting the phase of the B-pulse[29]. For rigid spectra with small τ_1 and τ_2 values the 'unwanted' FID generated by application of pulse lengths below 90° was removed by superimposing the solid echo and the spin alignment echo[31].

RESULTS

Spin relaxation times

The recovery of spin magnetization after saturation could clearly be separated into a rapid increase due to mobile deuterons in the amorphous regions of PE (see below) and a slow increase due to 'rigid' deuterons in the crystalline regions. The spin–lattice relaxation time T_1^c of the rigid deuterons was only determined for temperatures $T \geqslant 293$ K because of prohibitively long accumulation times at low temperatures, in particular, since relaxation became non exponential with an extremely long time tail that may be attributed to deuterons isolated from mobile defects. It should be noted that spin diffusion[32] is largely quenched by the quadrupole coupling in ^2H n.m.r. Thus, transport of spin energy to mobile sites[33] is ineffective for distances above a few Å[34]. At high temperatures, the T_1 values can be explained by motions connected with the α process except for the 180° flip motion that leaves the ^2H quadrupole coupling invariant[35]. Spin–lattice relaxation of the mobile deuterons in the amorphous regions (T_1^a) behaves very similar to that of protons in melt crystallized PE[33]. Thus, the T_1-minimum is at the same temperature of ~260 K for the Larmor frequency of 55 MHz, and the temperature dependence agrees within experimental accuracy. The absolute values, $T_1^{a,min}$ (^2H) = 20 ms and T_1^{min} (^1H) = 1.7 s[33] differ by a factor of 85 whereas the square of the quadrupole to dipole coupling ratio is 15 if only the dipole coupling between the CH_2 protons is considered[35]. Haeberlen[33] has assumed that kink motions (*trans–gauche* transitions) provide the basic mechanism for ^1H spin–lattice relaxation. By analysing the frequency dependence of the T_1 minimum in a range of Larmor frequencies between 22 and 88 MHz he concludes that spin diffusion to relaxation sinks influences the T_1 values. Since spin diffusion is difficult to handle quantitatively and moreover, the kink motion reorients H–H and C–H vectors, respectively, by different angles[36,37] a quantitative comparison of ^1H and ^2H spin–lattice relaxation times is difficult. If, on the other hand, our values of $T_1^a(^2H)$ are compared with ^{13}C relaxation times[38] the data agree within experimental accuracy provided the different coupling and shape of the spectral density is properly taken into account. This agreement should be expected since the same motions of the C–H vector determine the ^{13}C and the ^2H relaxation times.

The spin alignment relaxation time T_{1Q}^c of 'rigid' deuterons in the crystalline regions was determined using the pulse sequence BCD of *Figure 1*. τ_1 was set to 150 μs which is of the order of T_2^a the decay time of the solid echo amplitude for the mobile deuterons[29]. Thus, the decay of the alignment echo amplitude recorded as a function of τ_2 was determined only by the crystalline deuterons. At temperatures $T \gtrsim 350$ K no complete suppression of the mobile deuterons was possible, and we let $\tau_1 = 20\ \mu s$ at 393 K. It is apparent from *Figure 2* that at temperatures around 300 K the long time limit of the T_{1Q}^c decay agrees with T_1^c whereas it is more rapid closer to the melting point where $T_{1Q}^c \approx T_{1Q}^a$ but $T_1^c \gg T_1^a$. The reduction of T_{1Q}^c at high temperatures is not related with premelting phenomena[39,40] but can be explained in terms of small angle oscillations of the PE chains about their axes and will be discussed further below along with the τ_2-dependence of the alignment echo spectrum that is related with the non exponential decay of the echo amplitude. The corresponding τ_2-dependence for the mobile deuterons is also non-exponential, and is described by two T_{1Q}^a components in *Figure 2*. No unique decomposition in two exponentials was possible, and the datapoints just denote the upper and lower limits of a T_{1Q} distribution. Thus, the weight factor of *Figure 2b* only indicate whether the lower or upper region of this distribution is more

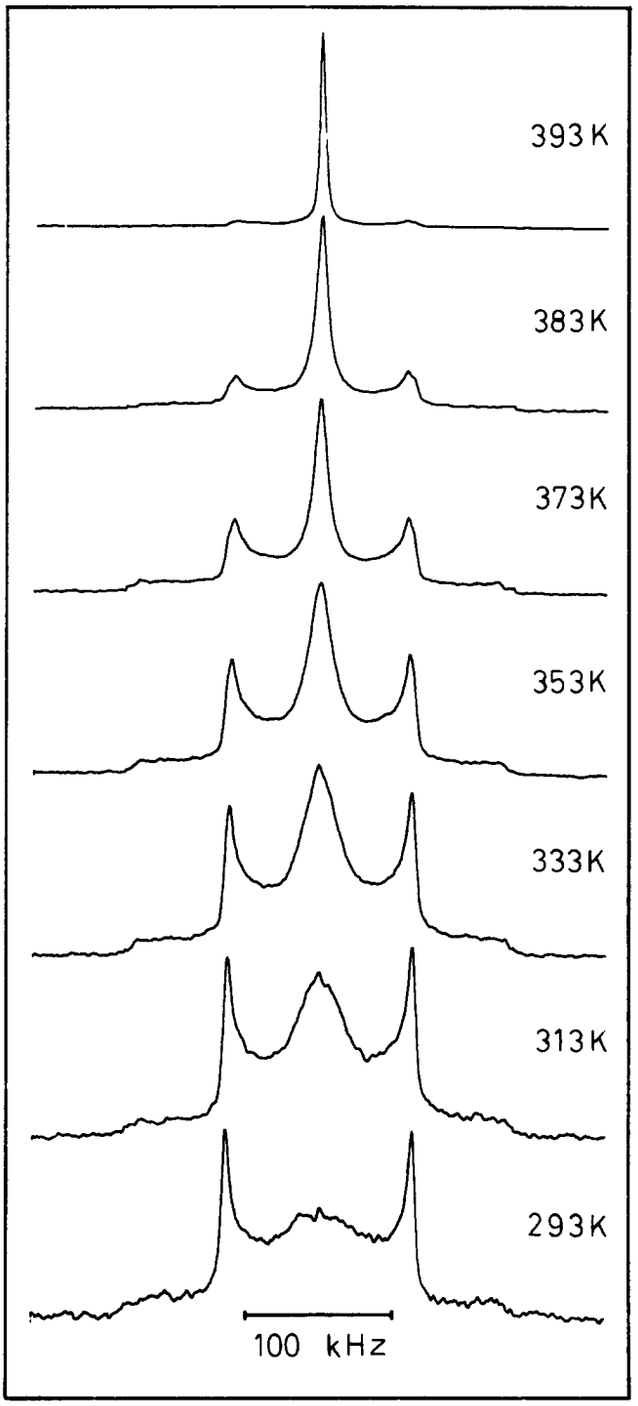

Figure 3 Fully relaxed ^2H solid echo n.m.r. spectra of polyethylene

populated. The upper limit of the T_{1Q}^a distribution agrees with that of T_1^a in the whole temperature region.

Crystallinity

The line shapes of fully relaxed solid echo spectra of PE (*Figure 3*) can be treated as a superposition of the Pake spectrum for rigid deuterons[1,35] and a motionally narrowed central region with decreasing widths at higher temperatures. The shape of the 'rigid' deuterons is also slightly changed at higher temperatures (see spectra at 373 and 383 K in *Figure 3*) thus indicating a finite asymmetry parameter η of the field gradient tensor. This feature has been analysed[35] in terms of torsional oscillations around the chain axis in the crystalline regions[20]. Since the shape of the rigid spectrum can readily be calculated a quantitative decomposition of the total spectrum in a rigid and a mobile portion is possible. In *Figure 4*, the mobile portion (b) was obtained by suppressing the rigid spectrum using the saturation recovery technique mentioned above. Subtraction from the total spectrum (a) yields the Pake spectrum (c) of rigid deuterons. Broadening of the Pake spectrum by deuteron dipolar coupling was taken into account in the calculated line shape[29]. This decomposition of the line shape in two components yields a rigid portion of $(77 \pm 5)\%$ very close to the X-ray crystallinity of 74% at 293 K. Since the height of the solid echo maximum is proportional to the number of excited spins the mobile (amorphous) fraction is equal to the ratio of echo heights of the partially relaxed over the fully relaxed deuterons where the partially relaxed echo is obtained by application of the pulse sequence ABC of *Figure 1* with $T_1^a \ll \tau_0 \ll T_1^c$, and $\tau_1 = 20$ μs is very short in comparison with T_2^a and T_2^c. These conditions apply in the temperature region between 293 and 353 K, and yield a constant rigid portion in agreement with the X-ray crystallinity. At higher temperatures, T_1^c decreases, and the inequality $T_1^a \ll \tau_0 \ll T_1^c$ breaks down. However, in this temperature region the line width of the mobile deuterons becomes rather narrow, and the ordinary free induction decay (FID) following a single 90° pulse can be recorded. This FID is dominated by the mobile deuterons in most of the time domain, and only slightly modulated by the rigid deuterons[29]. Thus, the mobile amorphous fraction could simply be determined from the amplitude of the FID after it was adjusted at 253 K to the value determined by the method applied in the low temperature region. The resulting decrease of the crystallinity at high temperature (*Figure 5*) agrees with an analysis of Raman and X-ray data[40].

Line shape of mobile deuterons

In *Figures 6* and *7*, the Fourier transform solid echo and spin alignment echo spectra, respectively, are shown for the mobile deuterons in PE. The contribution of the rigid deuterons was suppressed by the saturation recovery technique described above. At 123 K and $\tau_1 = 20$ μs, the line shape of the solid echo spectrum agrees with the Pake line shape of a rigid solid if we subtract the two small central peaks[2] due to <0.5% of the rotating methyl

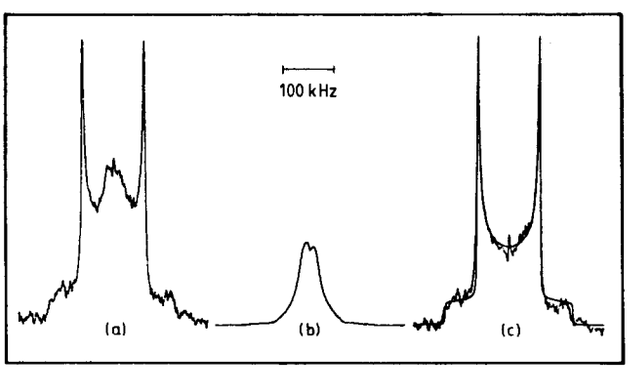

Figure 4 Decomposition of ^2H solid echo n.m.r. spectrum of PE at 293 K. (a) Fully relaxed spectrum. (b) Partially relaxed spectrum showing only the signal of mobile deuterons. (c) Difference spectrum (a–b) compared with computed Pake spectrum

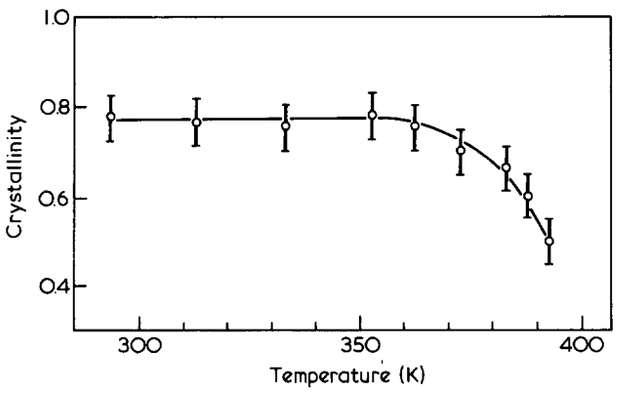

Figure 5 Crystallinity of polyethylene as determined by ^2H n.m.r.

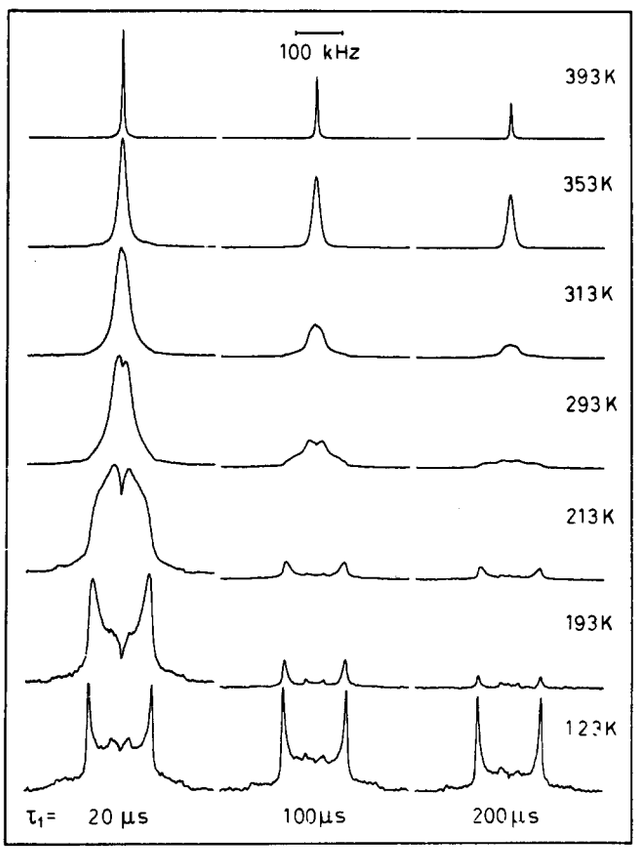

Figure 6 Solid echo n.m.r. spectra of mobile deuterons in polyethylene

groups present in the sample. At increased values of τ_1, an increasing amount of intensity is lost in the central region of the spectrum. This behaviour can be explained by a motional process that exchanges the C–H bond between two orientations differing by the tetrahedral angle[41]. Such a process must be related with *trans–gauche* transitions of the chain that are apparently present in PE at 123 K. The correlation time is of the order of 100 μs since at these τ_1-values the solid echo spectra are changed in the central region. However, this motion is only seen for about 1/3 of the non-crystalline deuterons since the solid echo spectra at 123 K yield only 7% of the total magnetization though the waiting time after saturation was $\tau_0 = 1$ s. The recovery was non-exponential at this temperature, and no meaningful value of T_1^a could be determined. The shape of the spin alignment echo spectrum at 123 K remains approximately the Pake spectrum for τ_2-values within 1–40 ms though some intensity is lost in this time domain, in particular, in the central region (*Figure 7*). This behaviour can be explained by 2 different processes, namely, 2 site exchange with correlation times of the order of 10 ms[29,42], or a more rapid small amplitude motion of the C–H vector that is restricted to a few degrees around the average position[43]. We favour the latter explanation since the former would imply a very broad distribution of correlation times for the 2 site exchange process that is at variance with our line shape calculations of the solid echo spectrum (see bwlow). The 'small amplitude' motion can also occur through a mechanism of rapid 2 site exchange where the jump angle fluctuates within a few degrees[43].

At 193 K, almost all non-crystalline deuterons were found to contribute to the solid echo spectrum though the waiting time after saturation was reduced to $\tau_0 = 80$ ms. The line shape differs markedly from the Pake spectrum for $\tau_1 = 20$ μs thus indicating that the correlation time is of this order of magnitude. We have tried to fit the solid echo spectra to theoretical spectra calculated for the model of 2 site exchange[1,29,41]. The shape of each of the spectra recorded for $\tau_1 = 20$, 100 and 200 μs, respectively, could be fitted with correlation times (inverse jump rates) around 50 μs[29].

However, a simultaneous fit of the 3 spectra with a single correlation time was not possible, in particular, the intensity reduction at higher τ_1-values was not properly described. The fit shown in *Figure 8* was achieved by a weighted superposition of theoretical shapes with correlation times τ_c between 20 and 100 μs and a jump

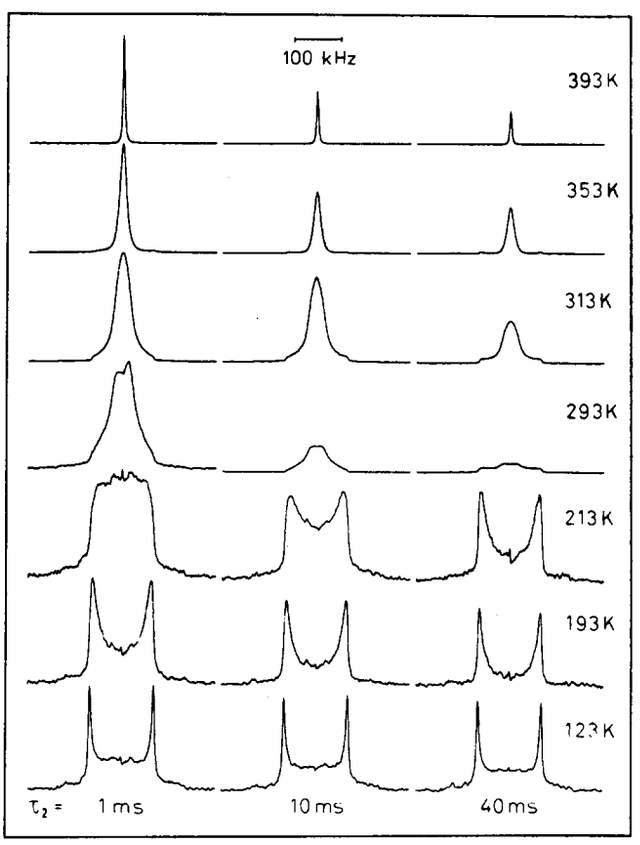

Figure 7 Spin alignment echo n.m.r. spectra of mobile deuterons in polyethylene. $\tau_1 = 20$ μs (160 μs at 293 K)

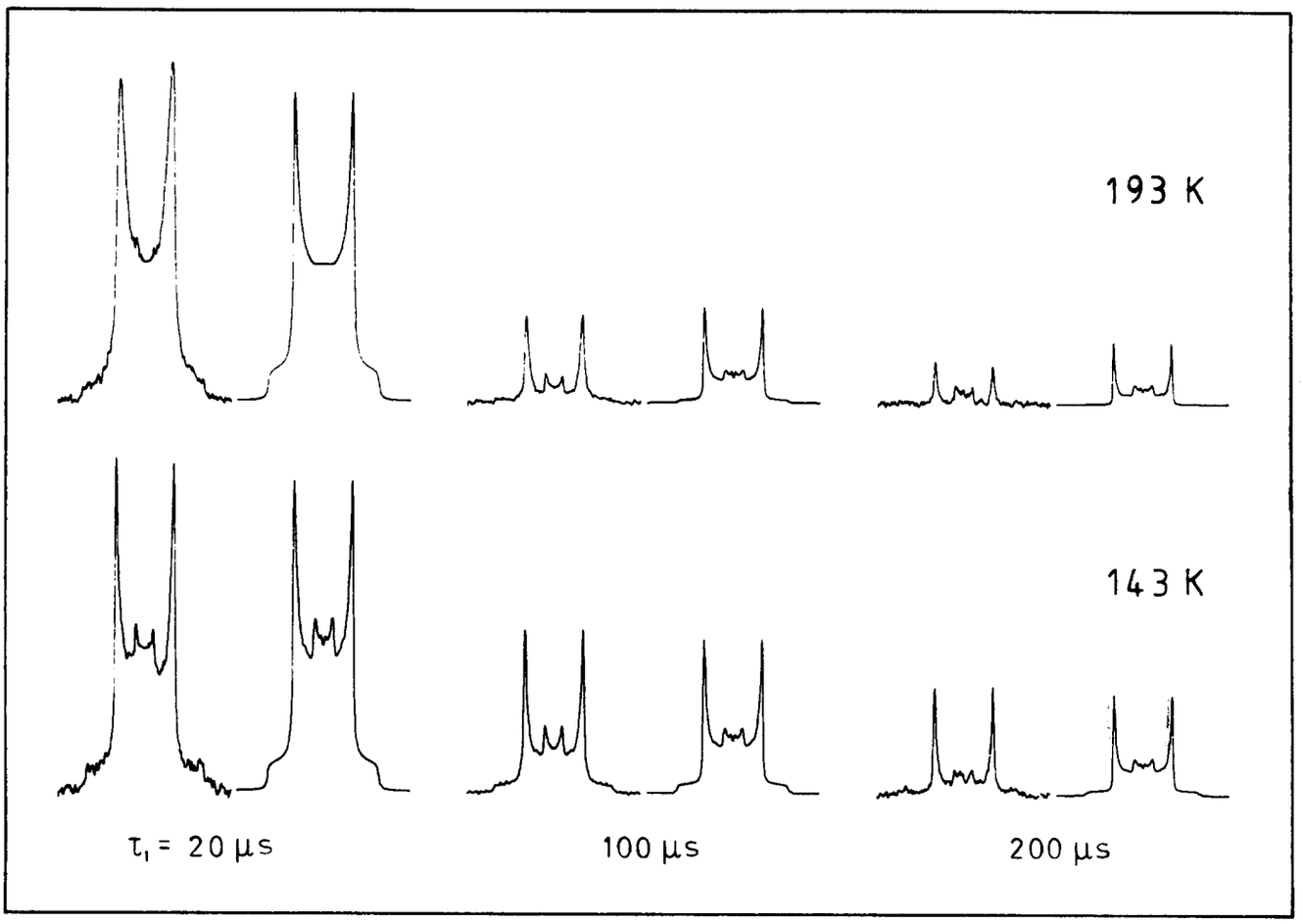

Figure 8 Observed and calculated solid echo n.m.r. spectra of mobile deuterons in polyethylene

angle of 111.5°C. For $\tau_1 = 20$ μs, the central region could only be fitted by including ~15% of the narrowed shape for $\tau_c \approx 0.1$ μs. This indicates the onset of another process where the C–H bond is exchanged between 3 possible orientations. At 143 K, a simultaneous fit of the 3 spectra shown in *Figure 8* was possible assuming 2 site exchange with a distribution of τ_c-values between 20 and 200 μs.

At 213 K, no superposition of theoretical shapes for 2 site exchange accounts for the solid echo spectra shown in *Figure 6*. However, an approximate fit is possible, if we assume that about 1/3 of the mobile deuterons are exchanged between 3 equally populated orientations. This is indicated in *Figure 9* by an area corresponding to a flexible unit of 5 bonds. At 293 K, this area has grown to about 2/3 of the mobile deuterons. It should be noted that these assignments refer to a weighted superposition of the 2 site and 3 site exchange process each having equally populated sites. An alternative model of exchange between 3 unequally populated sites should also explain the line shapes in this temperature regime. Furthermore, the motion of 3 and 5 flexible bond (*Figure 9*) refers to simulations on a diamond lattice[36] where the 2 site exchange corresponds to the kink 3-bond motion, and the 3 site exchange to the Schatzki crankshaft 5-bond motion. Recent simulations of carbon chain motion[44] suggest that rigorously cooperative 3- or 5-bond motions should not occur in free chains. Exchange between 4 sites is only possible in a diamond lattice if 7 or more bonds participate in the motion. In our previous simulations[36] we have related mobile chain portions between fixed

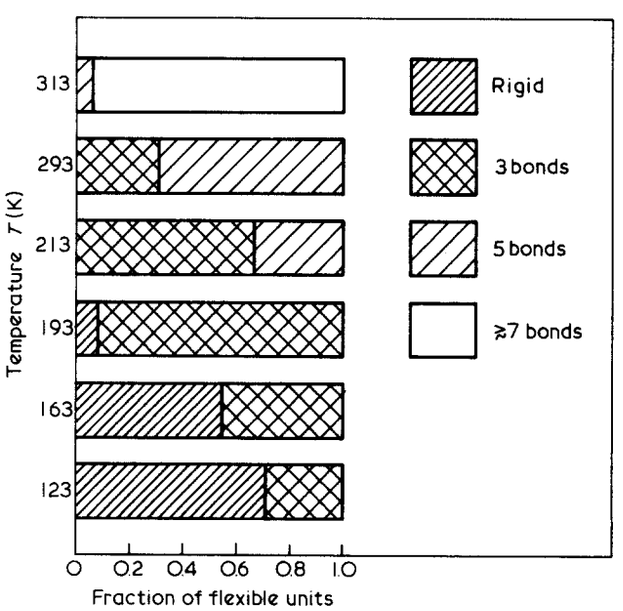

Figure 9 Fractions of flexible units in the non-crystalline regions of polyethylene as obtained from the analysis of solid echo n.m.r. line shapes

entanglement portions with the resulting line shapes in the rapid motion limit. In this model, the line shape is determined solely by the populations of the 4 tetrahedral orientations of the C–H bond. Thus, equal population of

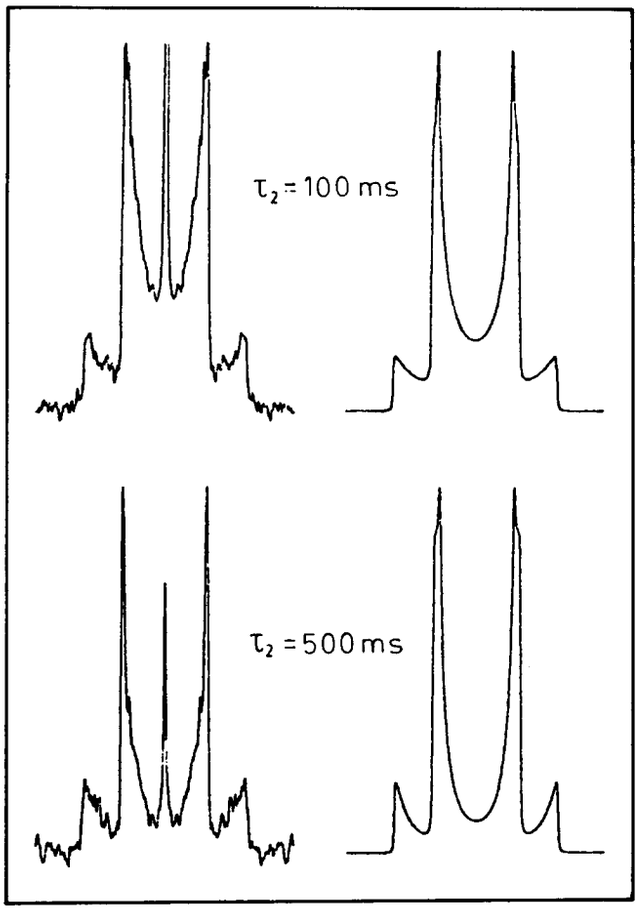

Figure 10 Observed and calculated spin alignment echo spectra at 393 K (see text). The spike in the centre is due to mobile deuterons in the amorphous regions

the 4 sites corresponds to zero line-width or fully isotropic rapid motion.

Though no correlation times can be obtained from solid echo line shapes in the rapid motion limit ($\tau_c \ll \tau_1$) the very fact that solid echoes and spin alignment echoes are detected in the non-crystalline regions of PE contains invaluable dynamics information. A solid echo can only be observed if the time averaged quadrupole coupling persists on the time scale of τ_1. At temperatures above about 230 K, the solid echo line-shape becomes independent of τ_1, and the decay of the total intensity is governed solely by the spin–relaxation time T_2 that determines the homogeneous widths of the spectra[29]. The spin alignment persists on a much longer time scale governed by the spin–lattice relaxation time T_1 at temperatures $T \gtrsim 213$ K. At 213 K, the shape of the spin–alignment echo spectrum is a function of τ_2 in the region of $1 \leqslant \tau_2/\text{ms} \leqslant 40$, (see *Figure 7*). This can be explained by the non-exponential T_1-decay in this temperature region. It is apparent from *Figure 2* that the rapid portion of the T_1^a- and R_{1Q}^a-decay amounts to $\sim 1/2$ of the mobile deuterons. If we assume that deuterons in the most flexible C–H bonds have the shortest relaxation times $T_1^a \lesssim 10$ ms and motionally narrowed spectra it is clear that the central portion of the spectrum shown in *Figure 7* should decay most rapidly. At higher temperatures the spin alignment shapes become independent of τ_2, and the intensity decays on the time scale of T_1^a (*Figures 2* and *7*). The result $T_{1Q}^a \approx T_1^a$ implies that the life time of the averaged quadrupole coupling is at least 40 ms even at 393 K just below the melting point where the 'crystallinity' is reduced to 50% (*Figure 5*).

Spin alignment spectra of crystalline deuterons

As noted above the decay time of the spin alignment echo decreases considerably at elevated temperatures (*Figure 2*). This is accompanied by characteristic line shape changes with increasing τ_2 as displayed in *Figure 10*. Two obvious reasons for this behaviour have to be considered:

(i) slow molecular motions on the time scale of τ_2;

(ii) frequency dependent spin–lattice relaxation of the alignment state.

We would like to show here that the latter can fully account for the line shape changes observed, provided the spin–lattice relaxation time of the alignment, T_{1Q}, is governed by rapid torisional oscillations around the chain axis[20,35]:

As shown in Ref. 31, $1/T_{1Q}$ is solely determined by the spectral density $g_{21}^Q(\omega_0)$ and $g_{2-1}^Q(=\omega_0)$ at the Larmour frequency ω_0, where the notation of Ref. 45 has been used. When calculating the spectral density for small angle oscillations, see also Ref. 46, it is readily shown that the spin–lattice relaxation rate is angular dependent:

$$\frac{1}{T_{1Q}} \propto \left(\frac{e^2qQ}{\hbar}\right)^2 \mathscr{D}_{01}^{(2)}(\alpha, \beta, 0)\mathscr{D}_{0-1}^{(2)}(\alpha, \beta, 0), \qquad (1)$$

where $e^2qQ/\hbar$ is the quadrupole coupling constant, $\mathscr{D}_{0\mp1}^2 = \mp\sqrt{3/8}\sin 2\beta e^{\mp i\alpha}$ are elements of the Wigner rotation matrix[45], and α, β are the Eulerian angles describing the orientation of the magnetic field $\vec{B}_0$ with respect to the C–H bond direction. Inserting $\mathscr{D}_{0\pm1}^{(2)}$ as given here we obtain:

$$\frac{1}{T_{1Q}}(\beta) \propto \left(\frac{e^2qQ}{h}\right)^2 \sin^2 2\beta \qquad (2)$$

Thus, $1/T_{1Q}$ depends only on the angle β between $\vec{B}_0$ and the C–H bond. Here we have neglected the fact that the oscillations also generate a finite asymmetry parameter. Then the n.m.r. frequency likewise depends on the angle β only:

$$\begin{aligned}\omega &= \omega_0 \pm \delta(3\cos^2\beta - 1) \\ &= \omega_0 \pm \omega_Q. \end{aligned} \qquad (3)$$

From this frequency dependence of $1/T_{1Q}$ is readily deduced:

$$\begin{aligned}1/T_{1Q}(\omega_Q) &\propto 2 - \omega_Q^2 + \omega_Q, \\ &(-1 \leqslant \omega_Q \leqslant 2),\end{aligned} \qquad (4)$$

which vanishes for $\omega_Q = -1$ and $\omega_Q = +2$, respectively. The theoretical line shapes presented in *Figure 10* were calculated from Equation 4. The agreement between observed and calculated spectra shows that frequency dependent spin–lattice relaxation can fully explain the line shape changes observed, at least at elevated temperatures, where the torsional oscilliations have a high amplitude[35]. Finally it should be noted that the frequency dependence of T_{1Q} calculated here, of course, also causes

non-exponential relaxation, if the echo amplitude is measured as a function of τ_2 as observed experimentally (*Figure 2*).

DISCUSSION

The main conclusions from our ^2H n.m.r. data can be summarized by saying that motion in the non-crystalline regions of PE is localized and highly constrained. In the low temperature regime of 120–190 K C–H bonds can only be exchanged between 2 possible orientations. At higher temperatures, an increasing number of C–H bonds gains access to the 3rd and above ~300 K to the 4th orientation inherent in the tetrahedral symmetry of carbon chain motion. The localized nature of the motion has been detected previously, in particular, by analysing dielectric relaxation in partially oxidized or chlorinated PE[15]. However, there must be additional constraints to the motion of the C=O or C–Cl dipoles since only 10–20% were found to participate whereas we have shown that all non-crystalline C–H bonds are mobile above ~190 K. We have described the constraints by a model where the carbon chain is restricted to a diamond lattice, and the number of fixed entanglement points is set at random along the model chain[36]. By comparing the experimental spectra with those calculated within this model we have determined the fractions and the lengths of flexible chain units given in *Figure 9*. Helfand and coworkers have recently performed Brownian dynamics simulations of polymer motion using a more realistic model chain[44,47]. The problem that a single *trans gauche* transition ($t \rightleftharpoons g^{\pm}$) necessitates a swing of a large polymeric tail is avoided by taking into account internal chain flexibility. Thus, the large distortion from a *trans–gauche* transition is cushioned by accompanying small distortions of neighbouring degrees of freedom, and asymptotically the tails remain stationary. However, the second neighbour is likely to perform cranklike counter-rotations shortly after occurance of a *trans–gauche* transition which then adds up to pair transitions $ttg^{\pm} \rightleftarrows g^{\pm}tt$ or $ttt \rightarrow g^{\pm}tg^{\mp}$. Attempts to describe our experimental results by this require additional assumptions that take account of the constraints that we have modelled as fixed entanglement points. Of course, the constraints must be related with intermolecular interactions and the fixation of chain ends in the crystalline regions of PE. It is remarkable that the necessary inclusion of 3 site exchange occurs in a temperature range above ~210 K (*Figure 9*) where the β transition is found by other experimental methods, and the line narrowing leading to almost isotropic 4 site exchange occurs above ~330 K (*Figures 3* and *6*) where the α process allows for chain rotation in the crystalline regions thus also relaxing constraints to motion in the non-crystalline regions.

It should be pointed out that most of our line shape results refer to the topology and yield only a lower limit for the life time of the constraints, namely, about 50 ms. From out deuteron T_1 values and those of ^1H [22,23] and ^{13}C [38] we know that the correlation times are below 10^{-7} s at $T \gtrsim 230$ K. Thus, we can only say that the number of conformations accessible to rapid motion increases on raising the temperature, but we know little about the shape of the time correlation functions. In principle, we could try to describe the spin–lattice relaxation times (*Figure 2*) and the line shapes in the slow motion regime (*Figure 8*) by particular non-exponential correlation functions or distributions of correlation times, and the corresponding activation energies. However, this might be misleading since the nature of the motional process changes as a function of temperature. Thus, our ^2H n.m.r. results suggest a different way of looking at motion in semicrystalline polymers. Rather than determining frequencies and activation energies of operationally defined $\alpha,\beta,\gamma,\ldots$ processes we obtain more detailed information about the nature of these processes on a molecular level, namely, of conformational transitions as seen from the reorientation of C–H bonds.

ACKNOWLEDGEMENT

Support by the Deutsche Forschungsgemeinschaft (Sonderforschungsbereich 41) is gratefully acknowledged.

REFERENCES

1 Spiess, H. W. *Colloid Polym. Sci.* 1983, **261**, 193
2 Hentschel, D., Sillescu, H. and Spiess, H. W. *Macromolecules* 1981, **14**, 1605
3 McCrum, N. G., Read, B. E. and Williams, G. 'Anelastic and Dielectric Effects in Polymeric Solids', John Wiley, London, 1967
4 Meier, D. J. (Ed.) 'Molecular Basis of Transitions and Relaxations', Midland Macromolecular Institute Monographs No. 4, 1976
5 Kitamaru, R. and Horii, F. *Adv. Polym. Sci.* 1978, **26**, 139
6 McBrierty, V. J. and McDonald, I. R. *Polymer* 1975, **16**, 125
7 Stehling, F. C. and Mandelkern, L. *Macromolecules* 1970, **3**, 242
8 Fischer, E. W. and Kloos, F. *J. Polym. Sci., Polym. Lett. Edn.* 1970, **8**, 685, and unpublished results
9 Davis, G. T. and Eby, R. K. *J. Appl. Phys.* 1973, **44**, 4274
10 Beatty, C. L. and Karasz, F. E. *J. Macromol. Sci., Rev. Macromol. Chem.* 1979, **17**, 37
11 Gauer, U. and Wunderlich, B. *Macromolecules* 1980, **13**, 445
12 Wunderlich, B. *J. Chem. Phys.* 1962, **37**, 2429
13 Pechold, W. and Blasenbrey, S. *Kolloid-Z.* 1967, **216/217**, 235
14 Schatzki, T. F. *Polym. Prepr., Am. Chem. Soc., Div. Polym. Chem.* 1965, **6**, 646
15 Ashchraft, Ch. R. and Boyd, R. H. *J. Polym. Sci., Polym. Phys. Edn.* 1976, **14**, 2153
16 Bergman, K. *J. Polym. Sci., Polym. Phys. Edn.* 1978, **16**, 1611
17 Klüver, W. and Ruland, W. *Progr. Colloid Polym. Sci.* 1978, **64**, 255
18 Kamel, I. and Charlesby, A. *J. Polym. Sci., Polym. Phys. Edn.* 1981, **19**, 803
19 Phaovibul, O., Loboda-Cackowic, J., Cackowic, H. and Hosemann, R. *Makromol. Chem.* 1974, **175**, 2991
20 Olf, H. G. and Peterlin, A. *J. Polym. Sci., Part A-2*, 1970, **8**, 753, 771
21 Kimmich, R. and Bachus, R. *Colloid Polym. Sci.* 1982, **260**, 911
22 Voigt, G. and Kimmich, R. *Polymer* 1980, **21**, 1001
23 Schaefer, J., Stejskal, E. O. and Buchdahl, R. *Macromolecules* 1977, **10**, 384
24 Dechter, J. J., Komoroski, R. A., Alexson, D. E. and Mandelkern, L. *J. Polym. Sci., Polym. Phys. Edn.* 1981, **19**, 631, and refs. therein.
25 VanderHart, D. L. *Macromolecules* 1979, **12**, 1232
26 Earl, W. L. and VanderHart, D. L. *Macromolecules* 1979, **12**, 762
27 Voelkel, R. *PhD Thesis*, University of Mainz, 1978
28 Hentschel, R. and Spiess, H. W. *J. Magn. Res.* 1979, **35**, 157
29 Hentschel, D. *PhD Thesis*, University of Mainz, 1981
30 Bloom, M., Davis, J. G. and Valic, M. I. *Can. J. Phys.* 1980, **58**, 1510
31 Spiess, H. W. *J. Chem. Phys.* 1980, **72**, 6755
32 Abragem, A. 'The Principles of Nuclear Magnetism', Oxford University Press, Oxford, 1961
33 Haeberlin, U. *Kolloid Z.u.Z.f.Polym.* 1968, **225**, 15 (1968)
24 Haeberlen, U., 24th Experimental NMR Conference, Asilomer 1983
35 Hentschel, D., Sillescu, H. and Spiess, H. W. *Makromol. Chem.* 1979, **180**, 241

36 Rosenke, K., Sillescu, H. and Spiess, H. W. *Polymer* 1980, **21**, 757
37 Rosenke, K. and Zachman, G. *Colloid Polym. Sci.* 1978, **64**, 238, 245
38 Dechter, J. J., Axelson, D. E., Dekmezian, A., Glotin, M. and Manderlkern L. *J. Polym. Sci., Polym. Phys. Edn.* 1982, **20**, 641
39 Strobl, G. R., Schneider, M. J. and Voigt-Martin, I. G. *J. Polym. Sci., Polym. Phys. Edn.* 1980, **18**, 1361
40 Fischer, E. W., Strobl, G. R. and Tanabe, Y. Jahresbericht 1978/79 des Sonderforschungsbereichs 41, p. 146, Mainz 1980
41 Spiess, H. W. and Sillescu, H. *J. Magn. Res.* 1981, **42**, 381
42 Lausch, M. and Spiess, H. W. *J. Magn. Res.*, in press
43 Rössler, E., Sillescu, H., Spiess, H. W. and Wallwitz, R. *Polymer* 1984, **25**, in press
44 Helfand, E., Wasserman, Z. R. and Weber, Th. A. *Macromolecules* 1980, **13**, 526
45 Spiess, H. W. in 'NMR, Basic Principles and Progress' (Eds P. Diehl, E. Fluck, and R. Kosfeld), Springer-Verlag, Berlin, 1978, Vol. 15, p 55
46 Torchia, D. A. and Szabo, A., *J. Magn. Res.* 1982, **49**, 107
47 Weber, Th. A. and Helfand, E. to be published